

## Chemical bonding and electronic structures of the $\text{Al}_2\text{SiO}_5$ polymorphs, andalusite, sillimanite, and kyanite: X-ray photoelectron- and electron energy loss spectroscopy studies

FUMIO S. OHUCHI,<sup>1</sup> SUBRATA GHOSE,<sup>2</sup> MARK H. ENGELHARD,<sup>3</sup> AND DONALD R. BAER<sup>3</sup>

<sup>1</sup>Department of Materials Science and Engineering, Box 352120, University of Washington, Seattle, Washington 98195, U.S.A.

<sup>2</sup>Department of Earth and Space Science, Box 351310, University of Washington, Seattle, Washington 98195, U.S.A.

<sup>3</sup>Pacific Northwest National Laboratory, Environmental Molecular Science Laboratory, Richland, Washington 99352, U.S.A.

### ABSTRACT

We have undertaken a detailed analysis of the X-ray photoelectron spectra obtained from the three polymorphs of  $\text{Al}_2\text{SiO}_5$ ; andalusite, sillimanite, and kyanite. Comparison of the spectra was made based on the chemical bonding and structural differences in the Al- and Si-coordination within each polymorph. The spectra for Si(2p) for all three polymorphs are nearly identical, consistent with the fact that all the Si atoms are in 4-fold (tetrahedral) coordination, whereas the binding energies, peak shapes, and peak widths for Al(2p) vary depending on the type of polymorph. The upper-valence band for all three polymorphs is characterized by four main features derived from O(2p), Al(3s), Al(2p), Si(3s), and Si(3p), and the differences in their contributions are observed. The density of state of the  $\text{Al}_2\text{SiO}_5$  polymorphs is relatively featureless compared to those observed from  $\alpha$ - $\text{SiO}_2$  and  $\alpha$ - $\text{Al}_2\text{O}_3$ , suggesting that the orbital overlaps span a greater range in energy. The observed band gap energy for  $\text{Al}_2\text{SiO}_5$  (sillimanite) was  $\sim 9.1$  eV, a value in between those for  $\alpha$ - $\text{SiO}_2$  ( $\sim 8.6$  eV) and  $\alpha$ - $\text{Al}_2\text{O}_3$  ( $\sim 9.6$  eV). The conduction band feature of  $\text{Al}_2\text{SiO}_5$  was experimentally compared to those of  $\alpha$ - $\text{SiO}_2$  and  $\alpha$ - $\text{Al}_2\text{O}_3$ , and shown that it is indeed intermediate between the  $\alpha$ - $\text{SiO}_2$  and  $\alpha$ - $\text{Al}_2\text{O}_3$  phases.

**Keywords:**  $\text{Al}_2\text{SiO}_5$  polymorphs, X-ray photoelectron spectroscopy, low electron energy loss spectroscopy, valence- and conduction band structures, andalusite, sillimanite, kyanite

### INTRODUCTION

The three polymorphs of  $\text{Al}_2\text{SiO}_5$ , sillimanite, andalusite, and kyanite, are geologically important minerals, whose crystal structures, and physical and thermodynamic properties have been extensively investigated (Kerrick 1990 and references therein). Crystal structures of sillimanite, andalusite, and kyanite were refined by Burnham (1963a), Burnham and Buerger (1961), and Burnham (1963b), respectively, following the structure determinations of kyanite by St. Naray Szabo et al. (1929), and sillimanite and andalusite by Taylor and Hey (1931). Further refinements of the sillimanite and andalusite structures were carried out using single-crystal neutron diffraction methods (Finger and Prince 1972). Winter and Ghose (1979) determined the thermal expansion and the structural changes of all three polymorphs as a function of temperature up to 1000 °C. The crystal structures of all three polymorphs have also been refined at high pressure [andalusite, Ralph et al. (1984); kyanite, Yang et al. (1997a) and Comodi et al. (1997); and sillimanite, Yang et al. (1997b)].

Sillimanite and andalusite are orthorhombic with space groups  $Pn\bar{m}$  and  $Pbnm$ , respectively, whereas kyanite is triclinic with  $P\bar{1}$ . The crystal structures of the three polymorphs have one feature in common, namely, half of the Al atoms occur in sixfold (octahedral) coordination forming chains of edge-shared  $[\text{AlO}_6]$  octahedra parallel to the crystallographic  $c$ -axis. The differences in their stability relations depend critically on the

differences in the chemical bonding of the remaining Al atoms in each polymorph: Al is in fourfold (tetrahedral) coordination in sillimanite (stable at low  $P$  and high  $T$ ), fivefold coordination (trigonal bipyramidal) in andalusite (stable at low  $P$  and low  $T$ ), and sixfold coordination (octahedral) in kyanite (stable at high  $P$  and high  $T$ ). The Si atom is in fourfold (tetrahedral) coordination in all three polymorphs. The reader is referred to the paper by Winter and Ghose (1979) for the details of the crystal structures of all three polymorphs.

Lattice dynamical studies of these minerals, including experimental measurements of phonon dispersion relations, density of states (DOS), and theoretical shell model calculations of their vibrational and thermodynamic properties, have been made by Rao et al. (1999). The electron density distributions in all three polymorphs have been determined experimentally from multipole refinements based on high resolution single crystal X-ray diffraction data collected at 100 K by a CCD detector (Dahaoui et al. 2001), and theoretically by ab initio quantum mechanical calculations using the LAPW method (Iglesias et al. 2001). The electric field gradient tensors at the  $^{27}\text{Al}$  sites in all three polymorphs calculated from the experimentally and theoretically derived electron density distributions match the values obtained from single-crystal  $^{27}\text{Al}$  NMR measurements (Raymond and Hafner 1970; Hafner et al. 1970; Hafner and Raymond 1967; Bryant et al. 1999).

The differences in the chemical bonding and electronic structures of the three  $\text{Al}_2\text{SiO}_5$  polymorphs are fundamental to the understanding of their thermodynamic properties and

\* E-mail: ohuchi@u.washington.edu

stability relations. X-ray photoelectron spectroscopy (XPS) is a technique to probe the chemical bonding of specific elements. However, application of the XPS technique to minerals, like the  $\text{Al}_2\text{SiO}_5$  polymorphs, is difficult due to sample charging during the analysis. Aleshin et al. (1975) used photoemission spectroscopy to reveal the nature of chemical bonding of the  $\text{Al}_2\text{SiO}_5$  polymorphs; however, as yet no systematic comparison of the chemical bonding for the three different polymorphs of  $\text{Al}_2\text{SiO}_5$  is available. Detailed analyses of photoelectron spectra obtained from alumino-silicate glass have been reported (Yagi et al. 2001; Miura et al. 2000). In glass form, however, Al and Si polyhedra are all corner linked, therefore the present study from three different polymorphs can give further insight into the chemistry and electronic structure of bonding about edge- and face-linked polyhedrons. We have undertaken an X-ray photoelectron spectroscopic study of the three  $\text{Al}_2\text{SiO}_5$  polymorphs to probe the differences in their chemical bonding, and compared the electronic structure of  $\text{Al}_2\text{SiO}_5$  (sillimanite) with those of  $\alpha\text{-SiO}_2$  (quartz) and  $\alpha\text{-Al}_2\text{O}_3$  (corundum) using proper charge compensation techniques. Low electron energy loss spectroscopy (LEELS) was also used to study the conduction band structure of the sillimanite phase of  $\text{Al}_2\text{SiO}_5$ .

## EXPERIMENTAL METHODS

Single-crystal samples of andalusite from Espiritu Santo, Brazil, sillimanite from Sri Lanka, and kyanite from Pizzo Forno, Switzerland were obtained from the Harvard Mineralogical Museum. Sample surfaces examined by XPS and LEELS were prepared by mechanically fracturing the samples in air, and mounted on a sample holder with indium solder. A typical duration for the fractured surface exposed in air (prior to evacuation in the sample load-lock chamber) was less than 30 min. The X-ray photoelectron spectroscopy experiments were performed using two different spectrometers: a modified SSL-300 spectrometer (Surface Science Laboratory Inc.) at the University of Washington, and a Quantum 2000 Scanning ESCA microprobe (Physical Electronics Inc.) at Pacific Northwest National Laboratories, Richland, Washington. In the first spectrometer, a focused monochromatic  $\text{AlK}\alpha$  X-rays with an X-ray spot of  $\sim 600$   $\mu\text{m}$  in diameter was used to measure core level data. In the second spectrometer, a monochromatic  $\text{AlK}\alpha$  X-ray beam ( $\sim 100$   $\mu\text{m}$  diameter) was rastered over an area of  $\sim 1.4$  mm by  $\sim 0.2$  mm on the specimen to collect valence band data. During analysis, charge neutralization was achieved by using a low energy (3–4 eV) electron flood gun. In the Quantum 2000 spectrometer, a low energy Ar-ion beam was applied in addition to the electron flood gun. All spectra were acquired using a pass energy of 50 eV with the SSL-300, and 23.5eV with the Quantum 2000 spectrometer. The binding energies were nominally calibrated using clean Cu and Au foils at  $\text{Cu } 2p_{3/2} = 932.72$  eV,  $\text{Cu } 3p_{3/2} = 75.10$ , and  $\text{Au } 4f_{7/2} = 83.98$  eV. In the analysis, the absolute value of the binding energy was calibrated by setting the C(1s) peak for the adventitious hydrocarbons accumulated on the surface at 284.60 eV.

For LEELS, the spectra were excited by unpolarized electrons with energies  $\sim 250$  eV incident normal to the surface, and were measured with a single pass cylindrical mirror analyzer (CAM). The current density of the incident electron beam was minimized to prevent electron beam damage of the sample surfaces. A pulse counting mode was used to collect the data. To obtain a constant system resolution, the full width at half maximum (FWHM) of the incident beam was set at a value of about 0.7 eV. For LEELS measurements, only a sillimanite sample was examined, and the results are compared to those from  $\alpha\text{-Al}_2\text{O}_3$  (corundum) and  $\alpha\text{-SiO}_2$  (quartz) phases. The binding energies of O(1s) found in  $\alpha\text{-Al}_2\text{O}_3$  and  $\alpha\text{-SiO}_2$  are 531.21eV and 532.54eV, respectively, which are similar to those reported previously (531.2eV for  $\alpha\text{-Al}_2\text{O}_3$  and 532.8eV for  $\alpha\text{-SiO}_2$ ) (Barr 1994).

## RESULTS AND DISCUSSION

### Si(2p) core-level spectra

The Si atoms in all three polymorphs are tetrahedrally bonded to O atoms, and form Al-O-Si linkages. The Si(2p) core level

spectra were carefully measured from sillimanite, andalusite, and kyanite, and compared with that measured from  $\alpha\text{-SiO}_2$  (Fig. 1). Analyses indicate that all the spectra reasonably fall into a single Gaussian peak with similar binding energy ( $E_b$ ) at around 102.28 eV (see Table 1), suggesting that the electronic environment around Si atoms in all three polymorphs of  $\text{Al}_2\text{SiO}_5$  and  $\alpha\text{-quartz}$  ( $\alpha\text{-SiO}_2$ ) is very similar, and that the second nearest-neighbor Al atoms do not significantly influence the electronic structure of the tetrahedrally-bonded Si atoms.

### Al(2p) core-level spectra

Figure 2 shows the Al(2p) spectra obtained from the three polymorphs. In kyanite, there are four symmetry-independent Al atoms present, all in octahedral coordination. The Al-O bond lengths vary within narrow limits (1.816 to 1.997 Å) (Winter and Ghose 1979); therefore, the Al(2p) peak is expected to be reasonably symmetric with a relatively narrow width. Curve fitting to a single Gaussian shape results in a peak maximum at  $74.48 \pm 0.05$  eV with FWHM of 1.68 eV (Fig. 2). Since the Al atomic arrangement in  $\alpha\text{-Al}_2\text{O}_3$  is also characterized by octahedral coordination with the Al-O bond lengths similar to those found in kyanite, Al(2p) spectra from kyanite and  $\alpha\text{-Al}_2\text{O}_3$  may be compared (Fig. 3). As shown in Fig. 3, the two Al(2p) peaks are nearly identical in terms of the relative binding energy. Note, however, that the Al(2p) peak from kyanite is slightly skewed in its low  $E_b$  tail, whereas a nearly perfect Gaussian peak was observed for  $\alpha\text{-Al}_2\text{O}_3$ . This small difference may be due to the influence of the second nearest-neighbor tetrahedral Si atoms in kyanite, and/or greater variation of the Al-O bond distances in kyanite (1.816 to 1.997 Å; Winter and Ghose 1979) vs.  $\alpha\text{-Al}_2\text{O}_3$  (1.857Å and 1.969 for short and long Al-O bond lengths, respectively; Chiang and Xu 1994).

The Al(2p) peak for sillimanite appears at a similar position in binding energy; however, the peak is considerably broader, and

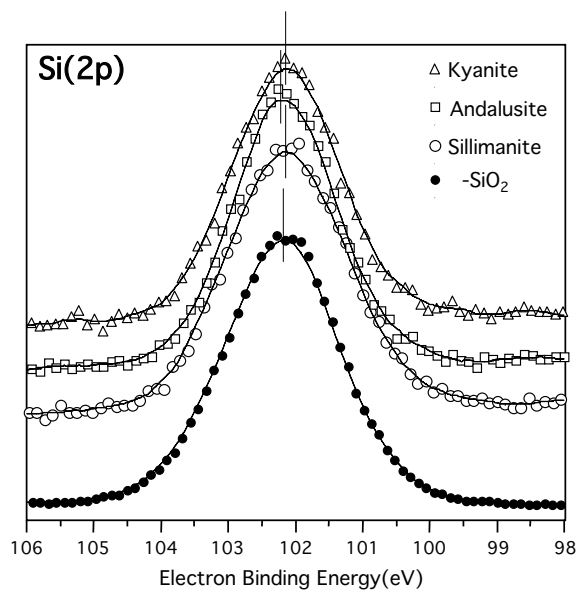
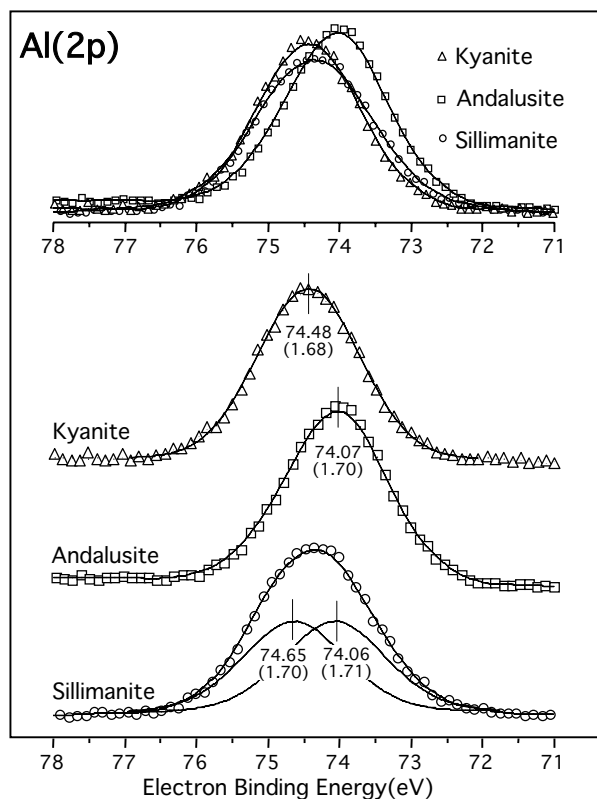


FIGURE 1. Si(2p) spectra obtained for sillimanite, andalusite, and kyanite, and comparison with Si(2p) of  $\alpha\text{-SiO}_2$ .

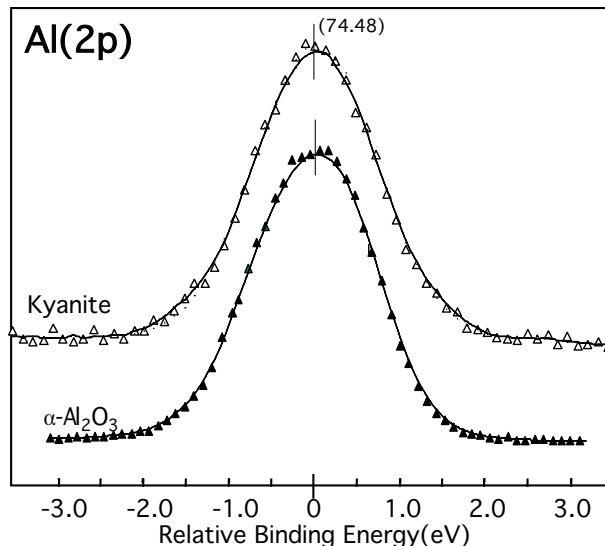
**TABLE 1.** Binding energy ( $E_b$  in eV), FWHM (eV) and relative fraction (%) for Si(2p), Al(2p), and O(1s) orbitals observed for the three polymorphs of  $\text{Al}_2\text{SiO}_5$ 

| Material                       | Si(2p)     |           |                     | Al(2p)     |           |                     | O(1s)      |           |                     |
|--------------------------------|------------|-----------|---------------------|------------|-----------|---------------------|------------|-----------|---------------------|
|                                | $E_b$ (eV) | FWHM (eV) | Relative fraction % | $E_b$ (eV) | FWHM (eV) | Relative fraction % | $E_b$ (eV) | FWHM (eV) | Relative fraction % |
| Kyanite                        | 102.27     | 1.81      | 100                 | 74.48      | 1.68      | 100                 | 531.39     | 1.97      | 80                  |
|                                |            |           |                     |            |           |                     | 530.59     | 1.98      | 20                  |
| Andalusite                     | 102.31     | 1.80      | 100                 | 74.07      | 1.70      | 100                 | 531.69     | 1.98      | 20                  |
|                                |            |           |                     |            |           |                     | 530.84     | 1.93      | 80                  |
| Sillimanite                    | 102.28     | 1.91      | 100                 | 74.65      | 1.70      | 50                  | 532.02     | 1.94      | 40                  |
|                                |            |           |                     | 74.06      | 1.71      | 50                  | 530.85     | 1.92      | 60                  |
| $\alpha\text{-SiO}_2$          | 102.28     | 1.92      | 100                 |            |           |                     | 532.54     | 1.95      | 100                 |
| $\alpha\text{-Al}_2\text{O}_3$ |            |           |                     | 74.48      | 1.78      | 100                 | 531.21     | 1.98      | 100                 |

**FIGURE 2.** Overlay of Al(2p) spectra observed from three polymorphs, and the results from curve fitting. See text for details.

the distribution extends toward the lower  $E_b$  side, suggesting two kinds of Al atoms: one similar to that in kyanite (more ionically bonded) and another less ionically bonded (or more covalently bonded). Based on the crystal structure of sillimanite (Winter and Ghose 1979), the Al atoms are in octahedral and tetrahedral coordination with equal fractions. We therefore fitted the curve to two peaks with their ratio constrained to 1:1 (Fig. 2c), resulting in  $E_b$  (FWHM) values 74.65 (1.70) and 74.06 (1.71). The analysis indicates that ~50% of the octahedrally coordinated Al atoms in sillimanite are slightly more ionic than those found in kyanite based on their binding energy values (75.65 eV for sillimanite vs. 74.48 eV for kyanite), whereas the other ~50% in tetrahedral coordination are less ionic ( $E_b$  ~74.06).

In the andalusite structure, the octahedral Al-coordination is severely distorted: four closely bonded O atoms within a square planar configuration with two each at 1.827 and 1.891 Å, and two farther apical O atoms at 2.086 Å (298 K) (Winter

**FIGURE 3.** Comparison of Al(2p) for kyanite and  $\alpha\text{-Al}_2\text{O}_3$ .

and Ghose 1979). The other Al atom in fivefold coordination is closely bonded to two O atoms at 1.814 Å and one at 1.816 Å forming a trigonal pyramid, while two further O atoms at 1.839 and 1.899 Å complete the trigonal bipyramid (298 K). In view of the structural complexity and hence, the complex nature of the chemical bonding, it does not seem justified to resolve the Al(2p) peak into contributions from the two types of Al atoms in distorted octahedral and the fivefold trigonal bipyramidal coordination. Therefore, we have fitted the Al(2p) spectra to a single peak. A reasonably good fit was found with a peak maximum at 74.06 eV with FWHM of 1.71 eV, as shown in Figure 2. These values are very similar to that for the tetrahedral Al atom in sillimanite ( $E_b$  74.06) (Table 1). Furthermore, the overall Al(2p) peak, shifted toward the lower binding energy by ~0.4 eV compared to kyanite ( $E_b$  74.48), suggests that the bonding for the Al atoms in andalusite is less ionic, compared to the octahedral Al atoms in either kyanite or sillimanite.

#### O(1s) core-level spectra

A set of O(1s) spectra obtained from three polymorphs is shown in Figure 4. The overall shapes of the O(1s) peaks observed in the three polymorphs are different. The chemical bonding of the O atoms with Al and Si in the  $\text{Al}_2\text{SiO}_5$  polymorphs is complex. Four symmetry non-equivalent O atoms are present in both andalusite and sillimanite, whereas kyanite has 10 non-equivalent O atoms. Since the charge density difference for each

oxygen atom may not vary significantly, we do not expect to be able to resolve all these binding energy differences; however, the overall shapes of the O(1s) peaks observed in the three polymorphs are different.

In kyanite, of the 20 O atoms in the unit cell, 16 are involved in Si-O-Al linkage, and 4 in Al-O-Al type linkages. The O atoms in the latter type are expected to be slightly more ionic than the former. We have therefore fitted the spectra with two Gaussian peaks with the ratio of 4:1, and obtained O(1s) peaks corresponding to Si-O-Al linkage (80%) and Al-O-Al linkage (20%) at 531.39 eV and 530.59 eV, respectively (see Table 1). Although the full-width at half-maximum (FWHM) of O(1s) peak ranges from 1.92 to 1.98 eV based on the Gaussian curve fitting, the separation of the peak maxima for the two-types of O(1s) is large enough to distinguish one peak from another.

The bonding differences in the various O atoms in sillimanite and andalusite can be analyzed in terms of the total charge each receives from the surrounding cations. In sillimanite, 12 O atoms are either charge balanced or slightly over bonded, and 8 are slightly under bonded. In andalusite, 4 are under bonded and 16 are either charge balanced or slightly over bonded. Following these considerations, the curve fittings for sillimanite and andalusite were made in 4:1, 2:3, and 1:4 ratios, respectively. Curve fitted results are shown for each polymorph in Figure 4 and Table 1. Our analysis indicates that 60% of the total O atoms

in sillimanite ( $E_b$ , 530.85) are more ionic compared to the other 40% ( $E_b$ , 532.02). This is consistent with the result obtained from Al(2p), in which one half of the total Al atoms is similar to those in kyanite, which is more ionic.

In andalusite, a major peak (>80% of the total) is centered around 530.84 eV, whereas <20% of the oxygen peak appeared with a peak maximum at 531.69 eV, suggesting that the majority of the O atoms are more ionic than those tetrahedrally bonded to Al in sillimanite (532.02). However, this result appears to be inconsistent with the Al(2p) value (74.07), which is comparable to that of tetrahedral Al in sillimanite (74.06). We currently do not have an explanation for this anomaly, and can only suggest that the explanation may lie in the structural complexity and hence, the complex nature of the chemical bonding of andalusite compared to that of kyanite and sillimanite.

### Valence-level spectra

Valence-level X-ray photoemission spectra are useful to characterize the nature of the chemical bonding, and may be directly compared with the electron density of state (DOS) calculations. In materials like  $\text{Al}_2\text{SiO}_5$ , an upper valence band (upper-VB) is characterized by a superposition of Al-Si-O hybridized orbitals and non-bonding O(2p) orbitals, whereas a lower valence band (lower-VB) is mainly due to O(2s) orbitals.

The upper-VB spectra obtained from the three different polymorphs of  $\text{Al}_2\text{SiO}_5$  are shown in Figure 5. The valence band width is very similar for all three phases, around ~11.0 eV, and the top of the valence band positions are all ~3.9 eV below the Fermi energy. Within the VB spectra, however, noticeable differences are observed from each polymorph, which are characterized by four main features labeled a, b, c, and d. The locations of these features in terms of  $E_b$  are similar, but the relative contributions vary for different polymorphs, obviously reflecting the types of bonding and coordination for Al, Si, and O atoms in the three polymorphs.

So far, the only DOS calculations available in the literature are those of Iglesias et al. (2001). These authors claimed that the cross-features of the DOS were similar for all atoms in all the three polymorphs. The total upper-VB DOS consists of mainly of O(2p), Al(3s), Al(2p), Si(3s), and Si(3p), in which the Si states appear at the lower energies, and the s-p splitting is more pronounced than for the corresponding Al states. All five orbitals are strongly mixed over the entire upper-VB regions. Note that Iglesias et al. (2001) assumed the top of the valence band as the Fermi-energy for the calculated partial density of states (PDOS), whereas the experimentally observed valence band starts around -4 eV in binding energy. In addition, the calculated binding energies are somewhat smaller than those observed experimentally, although the overall nature of the calculated and experimentally observed valence band structures is very similar.

Based on these calculations, the feature labeled a (around 5-6 eV in Fig. 5) consists of mainly O(2p) contribution with little overlap from the Si and Al orbitals. Feature b around 9 eV is the Si(2p and 3p) and Al(2p and 3s) overlapped with O(2p), whereas the s-orbitals from both Al and Si are not strongly involved. Feature c at around 11 eV is similar to b, but has more contribution from the Al(3s) orbitals; therefore, it varies for the three different polymorphs. In our measurements, this was seen

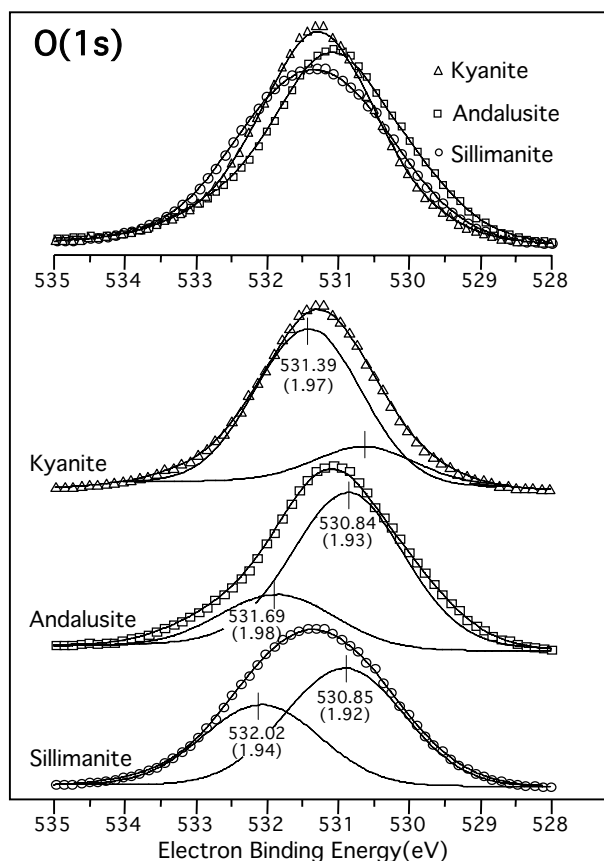


FIGURE 4. Overlay of O(1s) spectra observed from three polymorphs, and the results from curve fitting. See text for details.

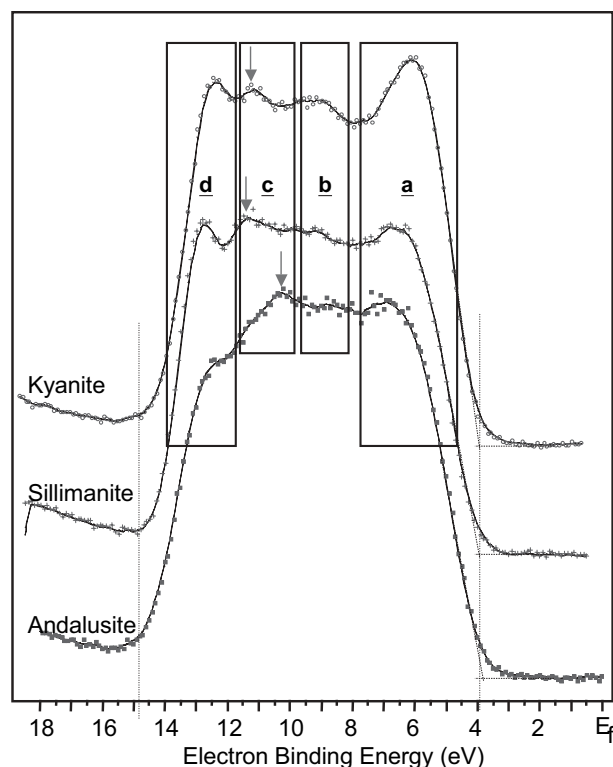


FIGURE 5. XPS valence band spectra from three polymorphs. See text for details about allows in the region c.

at different peak locations in the binding energy for sillimanite, kyanite, and andalusite [as represented by  $\downarrow$  (downward-pointing arrow) in Fig. 5]. The last feature labeled d originates mainly from Si(3s) orbitals, weakly overlapped with O(2p) orbitals. In andalusite, this feature d is much weaker than those found for kyanite and sillimanite, suggesting that the covalent nature of the Al-O type bonding is more dominant in this structure. This result is consistent with the fact that kyanite (which is stable at high pressure) has the highest coordination numbers for Al atoms in comparison to andalusite (6 and 5) and sillimanite (6 and 4), and hence an expected higher degree of ionic bonding. The higher ionic nature of Al in kyanite may be the reason why the feature “a” [O(2p) non-bonding] is more enhanced relative to sillimanite and andalusite. Note that a similar peak found in  $\alpha\text{-Al}_2\text{O}_3$  (feature “g” in Fig. 6) is also enhanced, which is consistent with the above interpretation. To confirm this, however, more detailed computations comparing three polymorphs are needed.

It has been suggested that a shift of the leading edge of O(2p) in the valence band toward the Fermi energy is a direct measure of increased ionicity in some materials (Barr 1991). However, we were unable to clearly identify a shift based on the leading edge positions observed in this study.

#### COMPARISON WITH QUARTZ ( $\alpha\text{-SiO}_2$ ) AND CORUNDUM ( $\alpha\text{-Al}_2\text{O}_3$ )

Electronic structures of quartz ( $\alpha\text{-SiO}_2$ ) and corundum ( $\alpha\text{-Al}_2\text{O}_3$ ) have been thoroughly investigated both experimentally and theoretically [for  $\alpha\text{-Al}_2\text{O}_3$ , see Siegel et al. (2002); Shang-Di and Chiang (1998) and references cited therein, and for

$\alpha\text{-SiO}_2$ , Gupta (1985); Di Pomponio et al. (1995) and references cited therein]. In quartz, Si atoms are tetrahedrally coordinated, whereas Al atoms in corundum are all octahedrally coordinated. In  $\text{Al}_2\text{SiO}_5$ , however, Al assumes different types of coordination depending on the polymorph. Therefore, it is worth comparing the occupied valence band (VB) and unoccupied conduction band (CB) spectra of  $\text{Al}_2\text{SiO}_5$  with its chemical components, namely,  $\alpha\text{-SiO}_2$  and  $\alpha\text{-Al}_2\text{O}_3$ . For comparison, we have chosen the sillimanite phase to represent the  $\text{Al}_2\text{SiO}_5$  polymorphs. In this structure, Al atoms are in both tetrahedral and octahedral coordination, whereas the Si atoms are tetrahedrally-coordinated. Figure 6 shows the XPS-VB spectra observed from  $\alpha\text{-SiO}_2$ , sillimanite and  $\alpha\text{-Al}_2\text{O}_3$ . Most noticeably, the upper-VB widths for the three materials are significantly different:  $\sim 13$  eV,  $\sim 11.5$  eV, and  $\sim 9$  eV for  $\alpha\text{-SiO}_2$ , sillimanite and  $\alpha\text{-Al}_2\text{O}_3$ , respectively. For both  $\alpha\text{-SiO}_2$  and  $\alpha\text{-Al}_2\text{O}_3$ , the upper-VB consists of mainly two features; a peak located at lower  $E_b$  side (labeled as e or g), and a peak at higher  $E_b$  side (labeled as f or h). Based on the DOS calculations, the features, e and g, are predominantly O(p)-non-bonding states with little contribution from O(s). These non-bonding states are spatially localized on the atomic sites and oriented transversally with respect to the Si-O and Al-O bonding direction for the quartz and corundum structures, respectively. The features at higher  $E_b$  side, f and h, mainly consist of strongly hybridized orbitals. The calculations indicate that these two features are well separated in both quartz and corundum, reflecting two distinct features found in calculated DOS (Iglesias et al. 2001). Observed DOS calculations for  $\text{Al}_2\text{SiO}_5$  are relatively featureless compared to those observed for  $\alpha\text{-SiO}_2$  and  $\alpha\text{-Al}_2\text{O}_3$ , suggesting that the orbital overlaps are much more spread out over the energy range, as previously described. It should also be pointed out that the valence band edges from the three materials occur nearly at the same binding energy ( $3.80 \pm 0.10$  eV).

The lower-VB spectra observed from the three materials are also shown in Figure 6. The DOS calculations reveal that the lower valence band is mainly O(2s) with small overlap from 2p-states associated with Si and/or Al. Thus, the differences in bonding and coordination are reflected in the peak locations and their shapes. The lower-VB spectra for sillimanite are similar to those of  $\alpha\text{-SiO}_2$  in terms of binding energies, but appear  $\sim 1$  eV higher than that for  $\alpha\text{-Al}_2\text{O}_3$ . Compared with O(1s) peaks, the lower VB peaks are considerably broader ( $\sim 4$  eV of FWHM), and therefore, detailed structures cannot be resolved. Nevertheless, this difference implies that the bonding character for sillimanite is more covalent than that of  $\alpha\text{-Al}_2\text{O}_3$ , but similar to that of  $\alpha\text{-SiO}_2$ .

Low energy electron loss spectroscopy (LEELS) is a technique for studying unoccupied states since the core electrons are excited into the unoccupied states in the conduction band (Koma and Ludeke 1975; Araki et al. 1976). Because the core states have well-defined energies and angular momenta, LEELS can probe the variation in the angular-momentum-resolved density of the conduction band state as joint density of states (JDOS). Shown in Figure 7 is LEELS spectra obtained from  $\alpha\text{-Al}_2\text{O}_3$ , sillimanite, and  $\alpha\text{-SiO}_2$ ; the spectra for  $\alpha\text{-Al}_2\text{O}_3$  and  $\alpha\text{-SiO}_2$  are excited from the Al(2p) and Si(2p) core levels, respectively, and for sillimanite from both Al(2p) and Si(2p) core levels. The LEELS spectra are then aligned by setting the threshold above 0 eV (Fermi energy) to an amount equal to the loss energy minus the corresponding

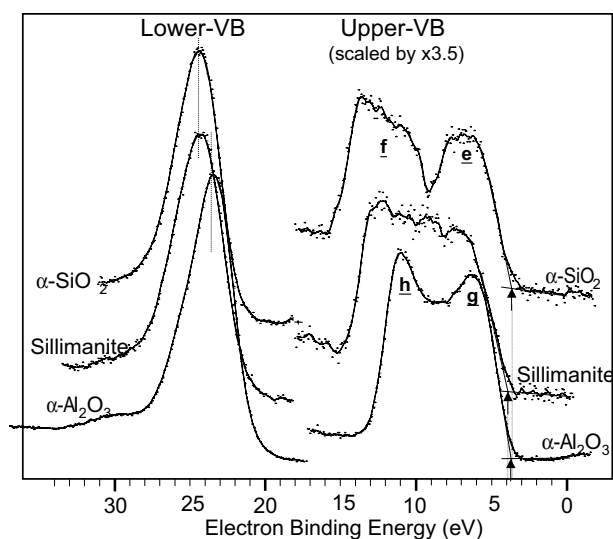


FIGURE 6. Comparison of the upper- and lower-valence bands from  $\alpha\text{-SiO}_2$ , sillimanite, and  $\alpha\text{-Al}_2\text{O}_3$ . The intensity of the upper-valence band was multiplied by 3.5.

core binding energy previously determined by XPS. The loss peak distribution above 0 eV represents JDOS of the conduction band. The onset energy of the JDOS corresponds to the energy difference between the bottom of the conduction band and the Fermi level of the material. The valence band edge occurs at  $3.80 \pm 0.10$  eV for all three materials. Therefore, the band gap energies for  $\alpha\text{-Al}_2\text{O}_3$ , sillimanite, and  $\alpha\text{-SiO}_2$  are determined to be  $\sim 9.6$  eV ( $3.8 + 5.8$ ),  $\sim 9.1$  eV ( $3.8 + 5.3$ ), and  $\sim 8.6$  eV ( $3.8 + 4.8$ ), respectively. Published values for the band gap ranges from 5.67 to 11.5 eV for  $\text{SiO}_2$  (Young-nian et al. and references therein) and from  $\sim 7$  to  $\sim 10$  eV for  $\text{Al}_2\text{O}_3$  (French et al. 1994; Gillet and Ealet 1992). Explanations for the range include the formation of excitons, presence of defects and temperature dependent Urbach tails. The band gap energy for  $\text{Al}_2\text{SiO}_5$ , sillimanite, is intermediate to those of  $\alpha\text{-Al}_2\text{O}_3$  and  $\alpha\text{-SiO}_2$ , which is reasonable based on the mixture of Si-O and Al-O bond configurations in these materials.

The JDOS spectra mainly consist of three primary regions labeled i (at  $\sim 4\text{--}8$  eV), j ( $\sim 10\text{--}15$  eV), and k ( $\sim 20\text{--}26$  eV) above the Fermi energy. Differences in the relative height for each region are related to the transition probability between the core and unoccupied conduction levels. Although transitions that give rise to the core-loss edge are governed by the atomic-dipole selection rules for electronic transitions, the spin-orbit split for Al(2p) and Si(2p) cannot be resolved in the present case. The resultant JDOS deduced from the LEELS, therefore, consists of all s-, p-, and d-like structures of the unoccupied states of the material. The region i for the three materials is similar, but the peak from  $\alpha\text{-SiO}_2$  is shifted toward higher energy. In the regions j and k for  $\alpha\text{-SiO}_2$  is less pronounced compared to  $\alpha\text{-Al}_2\text{O}_3$ . Sillimanite follows both features shown by  $\alpha\text{-SiO}_2$  and  $\alpha\text{-Al}_2\text{O}_3$ , implying that the conduction band for sillimanite is indeed intermediate to those of  $\alpha\text{-SiO}_2$  and  $\alpha\text{-Al}_2\text{O}_3$  phases. Given the broad nature of the conduction band for sillimanite, it is expected that the conduction bands in andalusite and kyanite should be similar to that found in sillimanite.

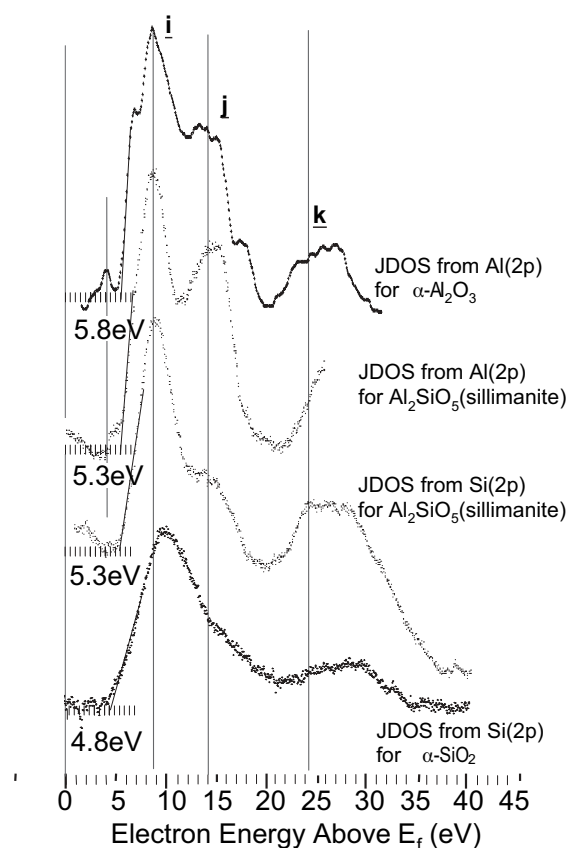


FIGURE 7. Comparison of the LEELS spectra obtained from  $\alpha\text{-SiO}_2$ , sillimanite, and  $\alpha\text{-Al}_2\text{O}_3$  by setting the threshold above 0 eV (Fermi energy) to an amount equal to the loss energy minus the corresponding core binding energy previously determined by XPS.

#### ACKNOWLEDGMENTS

We are indebted to Carl Francis, Harvard Mineralogical Museum, Cambridge, Massachusetts for the single-crystal samples of andalusite (Embilipitiya, Brazil HMM no. 129874), sillimanite (Sri Lanka), and kyanite (Pizzo Forno, Switzerland). Parts of the work were conducted in the Environmental Molecular Sciences Laboratory a DOE User Facility operated by Battelle for the DOE Office of Biological and Environmental Research.

#### REFERENCES CITED

- Aleshin, V.G., Dikov, Yu.P., Nemoshkalenko, V.V., Salova, T.P., Senkevich, A.I., Taldenko, Yu.D., Chichagov, A.V., and Epel'baum, M.B. (1975) Some results of an electron-spectroscopic investigation of silica. *Metallofizika* 60, 39 (in Russian).
- Araki, A., Nishikawa, S., Tanbo, T., and Tatsuyama, C. (1986) Low-energy electron-loss spectroscopy of GaSe and InSe. *Physical Review*, B33, 8164–8170.
- Barr, T. (1991) Recent advances in x-ray photoelectron spectroscopy studies of oxides. *Journal of Vacuum Science and Technology*, A9(3), 1793–1805.
- (1994) *Modern ESCA, The Principles and Practice of X-ray Photoelectron Spectroscopy*. CRC Press, Boca Raton, Florida.
- Burnham, C.W. (1963a) Refinement of the crystal structure of sillimanite. *Zeitschrift für Kristallographie*, 118, 127–148.
- (1963b) Refinement of the crystal structure of kyanite. *Zeitschrift für Kristallographie*, 118, 337–360.
- Burnham, C.W. and Buerger, M.J. (1961) Refinement of the crystal structure of andalusite. *Zeitschrift für Kristallographie*, 115, 269–290.
- Bryant, P.L., Harwell, C.R., Wu, K., Fronczek, F.R., Hall, R.W., and Butler, L.G. (1999) Single-crystal  $^{27}\text{Al}$  NMR of andalusite and calculated electric field gradients: the first complete NMR assignment for a 5-coordinate aluminum site. *Journal of Physical Chemistry A*, 103, 5246–5252.
- Chiang, W. Y. and Xu, Y.-N. (1994) First principle calculation of electronic, optical and structural properties of  $\alpha\text{-Al}_2\text{O}_3$ . *Journal of American Ceramic Society*, 77, 404–411.

- Comodi, P., Zanazzi, P.F., Poli, S., and Schmidt, M.W. (1997) High pressure behavior of kyanite: decomposition of kyanite into stishovite and corundum. *American Mineralogist*, 82, 460–466.
- Dahaoui, S., Ghermani, N.E., Ghose, S., and Howard, J.A.K. (2001) Electric field gradient tensors at the aluminum sites in the  $\text{Al}_2\text{SiO}_5$  polymorphs from CCD high resolution X-ray diffraction data: comparison with  $^{27}\text{Al}$  NMR results. *American Mineralogist*, 86, 159–164.
- Di Pomponio, A., Continenza, Lozzi, A.A., Passacantando, L., Santucci, M., and Picozzi, P. (1995) Electronic properties of crystalline and amorphous  $\text{SiO}_2$  investigated via all-electron calculations and photoemission spectroscopy. *Solid State Communications*, 95, 313–17.
- Finger, L.W. and Prince, E. (1972) Neutron diffraction studies: andalusite and sillimanite. *Carnegie Institution of Washington, Year Book*, 71, 496–500.
- French, R.H., Jones, D.J., and Loughlin, S.J. (1994) Interband electronic structure of alpha -alumina up to 2167 K. *Journal of the American Ceramic Society*, 77, 412–22.
- Gillet, E. and Ealet, B. (1992) Characterization of sapphire surfaces by electron energy-loss spectroscopy. *Surface Science*, 273, 427–436.
- Gupta, R.P. (1985) Electronic structure of crystalline and amorphous silicon dioxide. *Physical Review*, B32, 8278–8292.
- Hafner, S.S. and Raymond, M. (1967) Nuclear quadrupole coupling tensors of  $\text{Al}^{27}$  in kyanite. *American Mineralogist*, 52, 1632–1642.
- Hafner, S.S., Raymond, M., and Ghose, S. (1970) Nuclear quadrupole coupling tensors of  $^{27}\text{Al}$  in andalusite ( $\text{Al}_2\text{SiO}_5$ ). *Journal of Chemical Physics*, 52, 6037–6041.
- Hey, J.S. and Taylor, W.H. (1931) The co-ordination number of aluminium in aluminosilicates. *Zeitschrift für Kristallographie*, 80, 428–441.
- Iglesias, M., Schwarz, K., Blaha, P., and Baldomir, D. (2001) Electronic structure and electric field gradient calculations of  $\text{Al}_2\text{SiO}_5$  polymorphs. *Physics and Chemistry of Minerals*, 28, 67–75.
- Kerrick, D.M., Ed. (1990) *The  $\text{Al}_2\text{SiO}_5$  Polymorphs*, 22, 406 pp. *Reviews in Mineralogy*, Mineralogical Society of America, Chantilly, Virginia.
- Koma, A. and Ludeke, R. (1975) Core-Electron Excitation Spectra of Si,  $\text{SiO}$ , and  $\text{SiO}_2$ . *Physical Review Letters*, 35, 107–110.
- Miura, Y., Matsumoto, S., Nanba, T., and Akawawa, T. (2000) X-ray photoelectron spectroscopy of sodium aluminosilicate glasses. *Physics and Chemistry of Glasses*, 41, 24–31.
- Naray-Szabo, St., Taylor, W.H., and Jackson, W.W. (1929) The structure of cyanide. *Zeitschrift für Kristallographie*, 71, 117–130.
- Ralph, R.L., Finger, L.W. Hazen, R.M., and Ghose, S. (1984) Compressibility and crystal structure of andalusite at high pressure. *American Mineralogist*, 69, 513–519.
- Rao, M.N., Chaplot, S.L., Choudhury, N., Rao, K.R., Azuah, R.T., Montfrooji, W.T., and Bennington, S.M. (1999) Lattice dynamics and inelastic neutron scattering from sillimanite and kyanite  $\text{Al}_2\text{SiO}_5$ . *Physical Review*, B60, 12061.
- Raymond, M. and Hafner, S.S. (1970) Nuclear quadrupole coupling tensors of  $^{27}\text{Al}$  in sillimanite ( $\text{Al}_2\text{SiO}_5$ ). *Journal of Chemical Physics*, 53, 4110–4111.
- Shang-Di, Mo and Chiang, W.Y. (1998) Electronic and optical properties of *theta*- $\text{Al}_2\text{O}_3$  and comparison to *alpha*- $\text{Al}_2\text{O}_3$ . *Physical Review*, B57(24), 15219–15228.
- Siegel, D.J., Hector Jr., L.G., and Adams, J.B. (2002) Adhesion, atomic structure, and bonding at the  $\text{Al}(111)/\alpha\text{-Al}_2\text{O}_3(0001)$  interface: A first principles study. *Physical Review*, B65, 85415–85434.
- Winter, J.K. and Ghose, S. (1979) Thermal expansion and high temperature crystal chemistry of the  $\text{Al}_2\text{SiO}_5$  polymorphs. *American Mineralogist*, 64, 573–586.
- Yagi, T., Susa, M., and Nagata, K. (2001) Ionic character of oxygen and its local structure in silicate glass containing alumina. *Physics and Chemistry of Glasses*, 42 (4/5) 287–91.
- Yang, H., Downs, R.T., Finger, L.W., Hazen, R.M., and Prewitt, C.T. (1997a) Compressibility and crystal structure of kyanite at high pressure. *American Mineralogist*, 82, 467–474.
- Yang, H., Hazen, R.M., Finger, L.W., Prewitt, C.T., and Downs, R.T. (1997b) Compressibility and crystal structure of sillimanite,  $\text{Al}_2\text{SiO}_5$  at high pressure. *Physics and Chemistry of Minerals*, 25, 39–47.
- Young-nian, X. and Ching, W.Y., (1991) Electronic and optical properties of all polymorphic forms of silicon dioxide. *Physical Review*, B44, 11048–59.

MANUSCRIPT RECEIVED DECEMBER 24, 2004

MANUSCRIPT ACCEPTED JANUARY 3, 2006

MANUSCRIPT HANDLED BY KEVIN ROSSO